ON THE PLASTIC ZONE SIZE AND SHAPE DEPENDENCE ON THE NOMINAL STRESS IN FRACTURE MECHANICS

Habib Zambrano Rodriguez, habibzr@rdc.puc-rio.br
Jaime Tupiassú Pinho of Castro, jtcastro@mec.puc-rio.br
Marco Antonio Meggiolaro, meggi@mec.puc-rio.br
Pontifical Catholic University of Rio de Janeiro, Rua Marques de São Vicente 225, Gávea, Rio de Janeiro, RJ, Brazil

Summary. The estimates of the size and shape of the plastic zones, traditionally used in Linear Elastic Fracture Mechanics (LEFM), are based on the supposition that the stress intensity factor (SIF) K_I (or K_{II} or K_{III}) is the only necessary parameter to describe them. However, when the linear elastic stress analysis problem is solved in an Inglis plate, or the cracked infinite plate is analyzed using the stresses generated by the complete Westergaard function, it is verified that those traditional estimates significantly underestimate the position of the elastoplastic border. This happens because those solutions ignore the influence of the nominal stress on the stress field. However, as in most of the practical cases nominal stresses of up to 80% of the yielding strength are used, it is worthwhile to generate better estimates ahead for the plastic zones of the cracks, which are presented in this work.

Keywords: *Fracture Mechanics, plastic zone size, cracks*

1. INTRODUCTION

The border $pz(\theta)$ of the plastic zone around the tip of a crack under mode I can be estimated using only the linear elastic stresses generated by K_I, superimposing the effect of all stress components through Tresca or Mises, and equating the result with the yielding strength S_y (Anderson, 2005; Barson, 1987; Barson and Rolfe, 1999; Broek, 1986; Broek, 1988; Gdoutos, 2006; Sanford, 1997; Sanford, 2003; Whittaker *et al.*, 1992). To visualize the several elastoplastic borders of the several plastic zones $pz(\theta)$ that can be estimated, one can plot $pz_\sigma(\theta)/pz_0 = [f(\theta)]^2$ obtained from Tresca and Mises under plane stress, and repeat this exercise under plane strain plotting $pz_\varepsilon(\theta)/pz_0$ to compare them using the same scale. In this way, the plastic zone sizes calculated from Mises and Tresca in mode I are given by (Unger, 2001)

$$Mises\begin{cases} pz(\,plane-\sigma\,) = (\,K_I^2/2\pi S_y^2\,)\cdot cos^2(\,\theta/2\,)\cdot[\,1+3\,sin^2(\,\theta/2\,)] \\ pz(\,plane-\varepsilon\,) = (\,K_I^2/2\pi S_y^2\,)\cdot cos^2(\,\theta/2\,)\cdot[(\,1-2\nu\,)^2+3\,sin^2(\,\theta/2\,)] \end{cases} \tag{1}$$

$$Tresca\begin{cases} pz(\,plane-\sigma\,) = (\,K_I^2/2\pi S_y^2\,)\cdot cos^2(\,\theta/2\,)\cdot[\,1+|sin(\,\theta/2\,)|\,]^2 \\ pz(\,plane-\varepsilon\,) = (\,K_I^2/2\pi S_y^2\,)\cdot\begin{cases} cos^2(\,\theta/2\,)\cdot[\,1-2\nu+|sin(\,\theta/2\,)|\,]^2,\ |\theta|<\theta_1 \\ sin^2\theta,\ |\theta|\geq\theta_1\equiv 2\,sin^{-1}(\,1-2\nu\,) \end{cases} \end{cases} \tag{2}$$

But the development of Irwin's solution, obtained from Westergaard's stress function

$$\sigma_y = \sigma\cdot(x+a)/\sqrt{[(x+a)^2-a^2]} \cong \sigma a/\sqrt{(2ax)} = \sigma\sqrt{(\pi a)}/\sqrt{(2\pi x)} = K_I/\sqrt{(2\pi x)} \tag{3}$$

clearly shows that K_I only quantifies the stresses when x tends to zero. Because of this, the linear elastic stress field around the crack tips should be always written as

$$\sigma_{ij}(r\rightarrow 0,\,\theta) = [K_I/\sqrt{(2\pi r)}]\cdot f_{ij}(\theta) \tag{4}$$

It is because of this as well that it is necessary to question the validity of K_I as the stress controlling parameter in the residual ligaments, because the nominal stresses found there are larger than the remotely applied ones, which are used in the calculation of K_I and in the classic pz estimates). For instance, in a plate of width $2w$ with a central crack $2a$ under traction stress σ_n perpendicular to the crack (which is the nominal value used in K_I), the average nominal stress in the residual ligament rl is $\sigma_n/(1-a/w)$, and $\sigma_y(x\rightarrow w,\,\theta=0)$ should tend to the analytical value $\sigma_n/\sqrt{(1-a^2/w^2)}$, and not to σ_n. Besides, as the yielding safety factor $\phi_y = \sigma_n/S_y < 3$ in most of the real components, the elastoplastic plastic zone border $pz(r,\theta)$ certainly doesn't have r tending to zero. In summary, estimating the effect of σ_n on the plastic zone can be a complex task, but of course this doesn't justify the common practice of ignoring these effects, assuming that K_I describes the plastic zone independently of σ_n. The indiscriminate use of K_I in fact can generate inappropriate predictions, or even unacceptable ones in several important cases. The problem is that many of those predictions are used by the engineering community without major questioning. Therefore it is worthwhile to more carefully study some of the limitations of K_I. For instance, the stress σ_y generated by K_I doesn't balance the force acting on a strip of width $2w$ with a small central crack $2a$ (and two residual ligaments $rl = w - a$) under traction by σ_n, which induces in the strip the force $F = 2\sigma_n \cdot t \cdot w = 2\sigma_n t(a + rl)$, where t is the thickness of the strip. But the force F' estimated from the stress σ_y caused by $K_I = \sigma_n\sqrt{(\pi a)}$ (if $rl >> a$) is given by

$$F' = 2\int_0^{rl}\frac{\sigma_n\sqrt{\pi a}}{\sqrt{2\pi x}}\,t\,dx = \sigma_n t\sqrt{2a}\int_0^{rl}\frac{dx}{\sqrt{x}} \Rightarrow \frac{F}{F'} = \frac{2\sigma_n t(a+rl)}{2\sigma_n t\sqrt{2a\cdot rl}} = \frac{(1+rl/a)}{\sqrt{2rl/a}} \tag{5}$$

Therefore, F' cannot estimate F, because the errors would grow as the ratio rl/a increased. In other words, the opposite effect one would expect happens: as the K_I expression gets more accurate, in strips with $a << w$, the F' estimate gets worse, as shown in Fig. 1(a). This shows that estimates based only on "intuition" can be very deceitful in practice.

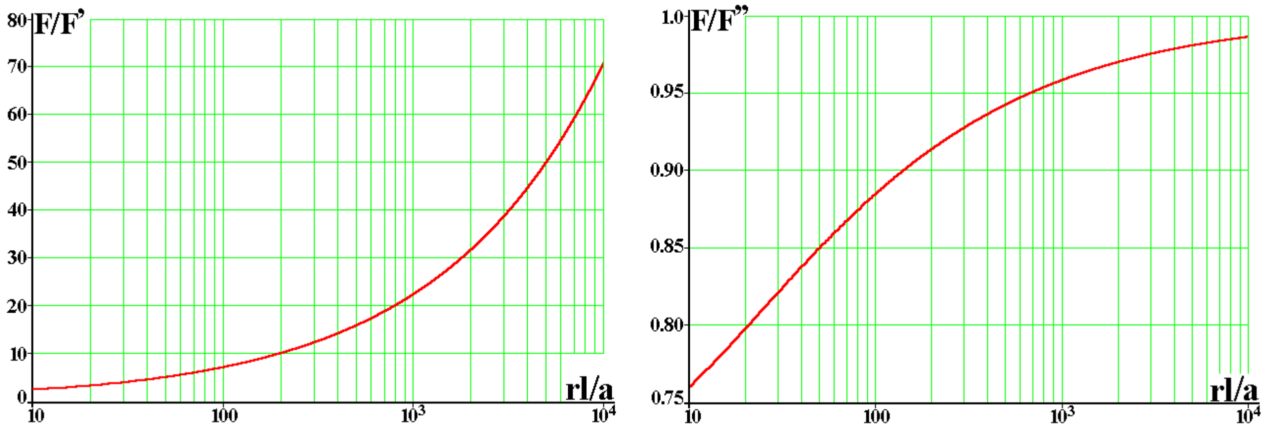

(a) (b)

Fig. 1: (a) Ratio $F/F' = (1 + rl/a)/\sqrt{(2rl/a)}$, where F is the actual traction force and F' is the force estimated from the σ_y stress generated by K_I in a strip with a central crack $2a$ and two residual ligaments rl; (b) $F/F'' \times rl/a$, where F'' is calculated from the sum of the stress σ_y generated by K_I and the nominal stress σ_n in the strip.

Irwin addressed the force balancing problem by translating σ_y, the stress generated by K_I, to compensate for the loss of force generated by the yielding at the plastic zone. However, his correction is not enough to balance the applied force in the piece, because it either doesn't satisfy the contour condition $\sigma_y(x \rightarrow \infty, 0) = \sigma_n$. An approximate way to satisfy this contour condition is to forcefully superimpose σ_n to the stress induced by K_I to obtain

$$\sigma_y = \frac{K_I}{\sqrt{2\pi r}}\cos\frac{\theta}{2}\left[1+\sin\frac{\theta}{2}\sin\frac{3\theta}{2}\right] + \sigma_n \tag{6}$$

This correction is simplistic, but it can generate interesting results, e.g. the force F'' that it generates in such strip is

$$F'' = 2\sigma_n t(\sqrt{2a\cdot rl} + rl) \Rightarrow \frac{F}{F''} = \frac{(1+rl/a)}{\sqrt{2rl/a} + rl/a} \tag{7}$$

The estimated F'' differs from the actual F that is applied to the strip by less than 25% for $10 \leq rl/a \leq 10^4$. In addition, it generates a significantly better estimate than the classical one (which neglects σ_n), as seen in Fig. 1(b). This problem can significantly influence the estimates for the plastic zone size and shape, which are the parameters that validate the LEFM predictions, as studied next.

2. NOMINAL STRESS INFLUENCE ON THE PLASTIC ZONE SIZE AND SHAPE

It is not difficult, at least, to estimate the effect of σ_n on the size and shape of the plastic zones, including its value in the elastoplastic border calculations under plane stress and plane strain. After doing this, it is found that the plastic zones are much larger than the ones estimated above, and they start to depend on the geometries of the piece and of the crack, and on the loading type. For instance, defining $\kappa = K_I/\sqrt{(2\pi r)}$, the Mises stress under plane stress when the condition $\sigma_y(x \rightarrow \infty, 0) = \sigma_n$ is applied is given by

$$\sigma_{Mises_{pl-\sigma}} = [(\kappa f_x)^2 + (\kappa f_y + \sigma_n)^2 - (\kappa f_x)(\kappa f_y + \sigma_n) + 3(\kappa f_{xy})^2]^{1/2} \tag{8}$$

where f_x, f_y and f_{xy} are the Williams' functions. The effect of σ_n on the plastic zone obtained from Mises under plane stress is calculated equating $\sigma_{Mises,pl-\sigma}$ and S_y, and solving this equation to obtain the function of θ that locates the elastoplastic border, see Fig. 2(a).

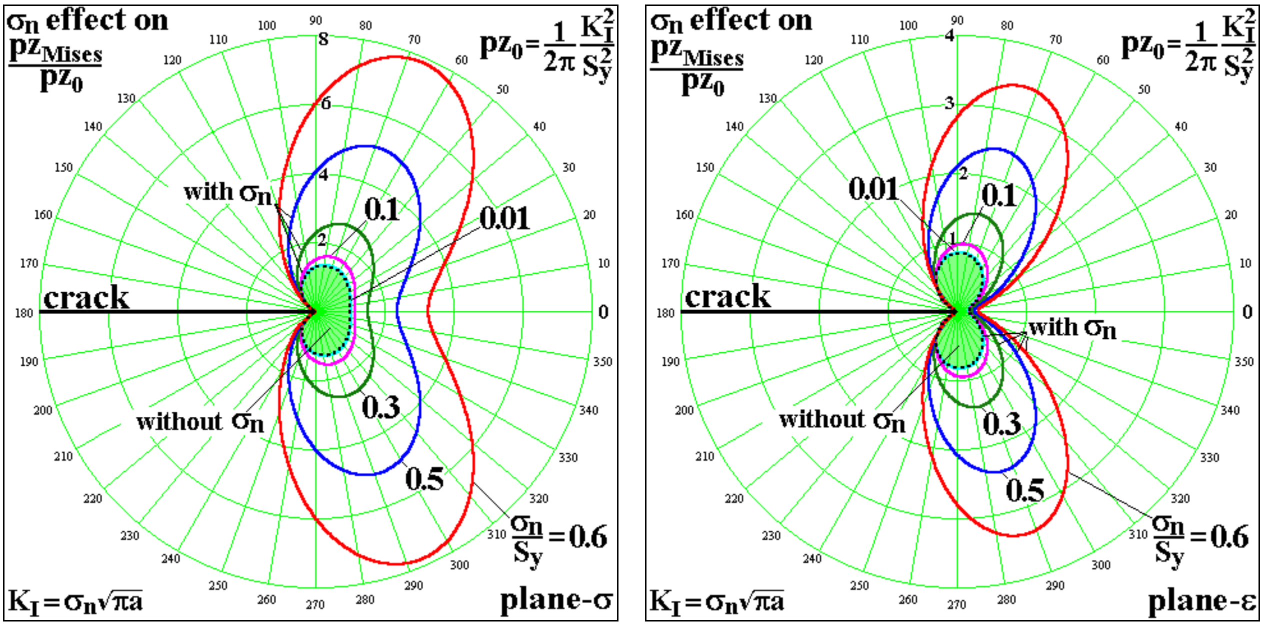

(a) (b)

Fig. 2: (a) The size and shape of the plastic zone estimated from Mises changes a lot when σ_n is added to Williams' σ_y, to force $\sigma_y \to \sigma_n$ far away from the crack tip (infinite plate with crack $2a$ under mode I and plane stress); (b) the effect of σ_n is also very large when this technique is used to estimate the plastic zones under plane strain.

It is easy to obtain similar expressions for σ_{Mises} under plane strain, see Fig. 2(b), and for σ_{Tresca} under plane stress and plane strain. These expressions depend on the geometry of the piece, because they include independent terms that cannot be eliminated when dividing K_I by a reference stress such as $\sigma_{Mises}(0)$, as seen in the previous models. Since yielding safety factors $1.5 < \phi_y < 3$ are common in practice, the influence of the nominal stress on the plastic zone shape and size is not just an academic curiosity. Actually, it is difficult to explain why this very significant effect of σ_n on the plastic zone is not properly emphasized in the literature, since it is the ratio between the plastic zone size and the piece dimensions (crack size a, residual ligament $rl = w - a$, thickness t, etc.) that validate LEFM predictions.

3. INGLIS' PLASTIC ZONE ESTIMATES

To more accurately estimate the elastoplastic border of the plastic zone in an infinite plate with a crack $2a$ under traction stress $\sigma_y(x, y \to \infty) = \sigma_n$, the Inglis' solutions or a complete Westergaard function can be used, because both consider all the problem contour conditions. This task is quite lengthy, but it is not particularly difficult. The Inglis' solution for the linear elastic stress field in an infinite plate under traction with a central elliptic hole can describe the stresses in an infinite plate with a central crack. To do this, the crack faces should coincide with the longer axis of the elliptic hole, with a tip radius that should be half of the CTOD. The Inglis' solution uses elliptic-hyperbolic orthonormal coordinates (α, β), which map the plane through ellipses generated from the coordinate α and through hyperboles generated from β, all of them with focus on $x = \pm c$, which are given respectively by

$$x^2/\cosh^2\alpha + y^2/\sinh^2\alpha = c^2 \quad \text{and} \quad x^2/\cos^2\beta - y^2/\sin^2\beta = c^2 \tag{9}$$

The Cartesian coordinates (x, y) relate to the elliptic-hyperbolic coordinates (α, β) by $x = c\cdot\cosh\alpha\cdot\cos\beta$ and $y = c\cdot\sinh\alpha\cdot\sin\beta$. The semi-axes of the elliptic hole whose border is given by $\alpha = \alpha_0$ are $a = c\cdot\cosh\alpha_0$ and $b = c\cdot\sinh\alpha_0$ (therefore $b/a = \tanh\alpha_0$), where $c = a/\cos\alpha_0$, and the hole is described by

$$x^2/\cosh^2\alpha_0 + y^2/\sinh^2\alpha_0 = c^2 \tag{10}$$

The stress component σ_α is perpendicular and the component σ_β is tangent to the ellipses α, in the direction that β varies, therefore they work in a similar way as polar components σ_r and σ_θ, respectively. In the general case, the stresses according to Inglis are given by

$$\begin{cases} \sigma_\alpha = \dfrac{1}{(\cosh 2\alpha - \cos 2\beta)^2} \sum_n A_n\{ (n+1)e^{(1-n)\alpha} \cos(n+3)\beta + (n-1)e^{-(n+1)\alpha} \cos(n-3)\beta - \\ \quad - [4e^{-(n+1)\alpha} + (n+3)e^{(3-n)\alpha}] \cos(n+1)\beta + [4e^{(1-n)\alpha} + (3-n)e^{-(n+3)\alpha}] \cos(n-1)\beta \} + \\ \quad + B_n\{ e^{-(n+1)\alpha} [n\cos(n+3)\beta + (n+2)\cos(n-1)\beta] - [(n+2)e^{(1-n)\alpha} + ne^{-(n+3)\alpha}] \cos(n+1)\beta \} \\ \sigma_\beta = \dfrac{1}{(\cosh 2\alpha - \cos 2\beta)^2} \sum_n A_n\{ (3-n)e^{(1-n)\alpha} \cos(n+3)\beta - (n+3)e^{-(n+1)\alpha} \cos(n-3)\beta - \\ \quad - [4e^{-(n+1)\alpha} - (n-1)e^{(3-n)\alpha}] \cos(n+1)\beta + [4e^{(1-n)\alpha} + (n+1)e^{-(n+3)\alpha}] \cos(n-1)\beta \} - \\ \quad - B_n\{ e^{-(n+1)\alpha} [n\cos(n+3)\beta + (n+2)\cos(n-1)\beta] - [(n+2)e^{(1-n)\alpha} + ne^{-(n+3)\alpha}] \cos(n+1)\beta \} \\ \tau_{\alpha\beta} = \dfrac{1}{(\cosh 2\alpha - \cos 2\beta)^2} \sum_n A_n\{ (n-1)e^{(1-n)\alpha} \sin(n+3)\beta + (n+1)e^{-(n+1)\alpha} \sin(n-3)\beta - \\ \quad - (n+1)e^{(3-n)\alpha}] \sin(n+1)\beta - (n-1)e^{-(n+3)\alpha}] \sin(n-1)\beta \} - \\ \quad - B_n\{ e^{-(n+1)\alpha} [n\sin(n+3)\beta + (n+2)\sin(n-1)\beta] - [(n+2)e^{(1-n)\alpha} + ne^{-(n+3)\alpha}] \sin(n+1)\beta \} \end{cases} \quad (11)$$

In the plate under uniaxial stress σ_n perpendicular to the a axis of the elliptic hole, only five constants of Inglis' series are not null:

$$A_1 = -\sigma_n(1 + 2e^{2\alpha_0})/16, \quad A_{-1} = \sigma_n/16, \quad B_1 = \sigma_n e^{4\alpha_0}/8, \quad B_{-1} = \sigma_n(1 + \cosh 2\alpha_0)/4, \quad \text{and} \quad B_{-3} = \sigma_n/8 \quad (12)$$

Because the border of the hole is a free surface, $\sigma_\alpha(\alpha = \alpha_0) = \tau_{\alpha\beta}(\alpha = \alpha_0) = 0$, and as at the border $\alpha_0 = \text{atanh}(b/a)$, the stress $\sigma_\beta(\alpha = \alpha_0)$ tangent to the border is given by

$$\sigma_\beta(\alpha=\alpha_0) = \sigma_n e^{2\alpha_0}\left[\frac{(1+e^{-2\alpha_0})\sinh 2\alpha_0}{\cosh 2\alpha_0 - \cos 2\beta} - 1\right] \quad (13)$$

Therefore, the stress $\sigma_\beta(\alpha = \alpha_0)$ is maximized at the end points of the axis $2a$ perpendicular to the applied load σ_n, where $\cos 2\beta = 1$ (thus $\beta = 0$ or π), where

$$\frac{\sigma_{\beta max}}{\sigma_n} = e^{2\alpha_0}\left[\frac{(1+e^{-2\alpha_0})\cdot\sinh 2\alpha_0}{\cosh 2\alpha_0 - 1} - 1\right] = \frac{3\dfrac{a+b}{a-b} - \dfrac{a-b}{a+b} - 2}{\dfrac{a+b}{a-b} + \dfrac{a-b}{a+b} - 2} = 1 + 2\frac{a}{b} \quad (14)$$

because $\dfrac{b}{a} = \tanh\alpha_0 = \dfrac{e^{\alpha_0} - e^{-\alpha_0}}{e^{\alpha_0} + e^{-\alpha_0}} \Rightarrow e^{2\alpha_0} = \dfrac{a+b}{a-b}$. In this way, being $\rho = b^2/a$ the radius of the elliptic hole at the two ends of its longer axis $2a$, perpendicular to the nominal stress σ_n, then

$$\frac{\sigma_{\beta max}}{\sigma_n} = K_t = 1 + 2\frac{a}{b} = 1 + 2\sqrt{\frac{a}{\rho}} \quad (15)$$

Assuming $\rho = CTOD/2 = 2K_I^2/\pi E' S_y$, and knowing that $K_I = \sigma_n\sqrt{(\pi a)}$, it can be seen that

$$\rho = \frac{2\cdot\sigma_n^2\cdot a}{E'\cdot S_y} \Rightarrow 1 + 2\cdot\frac{a}{b} = 1 + 2\cdot\sqrt{\frac{E'\cdot S_y}{2\cdot\sigma_n^2}} \Rightarrow \frac{a}{b} = \sqrt{\frac{E'}{2\cdot\sigma_n}\cdot\frac{S_y}{\sigma_n}} \quad (16)$$

Using the yielding safety factor $\phi_y = S_y/\sigma_n$ in the equation above, then

$$\begin{cases} \dfrac{b}{a} = \sqrt{\dfrac{2}{\phi_y^2}\dfrac{S_y}{E}}, \quad plane-\sigma \\ \dfrac{b}{a} = \sqrt{\dfrac{2}{\phi_y^2}\dfrac{S_y(1-\nu^2)}{E}}, \quad plane-\varepsilon \end{cases} \tag{17}$$

Substituting the constants given in Eq. (12) into Eq. (11) to obtain the Inglis' stresses in an infinite cracked plate under traction σ_n, the elastoplastic *pz* border can then be mapped around the crack tip using semi-axes given by Eq. (17). Using Mises under plane stress, the following equation should be solved:

$$\sigma_{Mises\,pl-\sigma} = \sqrt{\sigma_\alpha^2 + \sigma_\beta^2 - \sigma_\alpha\sigma_\beta + 3\tau_{\alpha\beta}^2} = S_y \tag{18}$$

Equation (18) can be solved numerically for α and β by fixing one of the variables first and then finding the value of the other one that leads to $\sigma_{Mises} = S_y$. To plot these points in polar coordinates, as shown in Fig. 3(a), (α, β) are first transformed into Cartesian coordinates (*x*, *y*), and then into polar coordinates (*r*, θ). The traditional plastic zone $pz(K_I)$ is given by Eq. (1), which only depends on K_I, not considering the effect of σ_n on the *pz* size and shape.

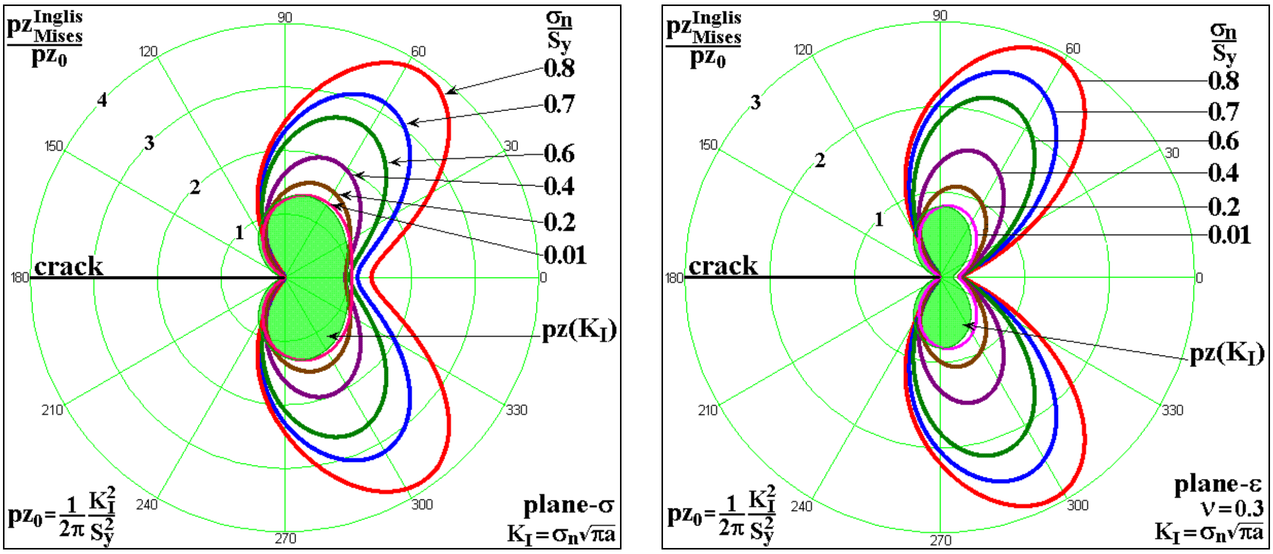

(a) (b)

Fig. 3: Plastic zones around the crack tip modeled as an Inglis' hole with ρ = *CTOD*/2 under: (a) plane stress; (b) plane strain.

In the plane strain case, the Mises stress near the crack tip is given by

$$\sigma_{Mises\,pl-\varepsilon} = \sqrt{0.5[(\sigma_\alpha - \sigma_\beta)^2 + (\sigma_\alpha - \sigma_z)^2 + (\sigma_z - \sigma_\beta)^2] + 3\tau_{\alpha\beta}^2} = S_y \tag{19}$$

where $\sigma_z = \nu(\sigma_\alpha + \sigma_\beta)$. A few elastoplastic borders generated from this equation are shown in Fig. 3(b).

4. WESTERGAARD'S PLASTIC ZONE ESTIMATES

To estimate the plastic zones considering the effect of the nominal stress in the cracked infinite plate, with a uniaxial traction stress σ_n perpendicular to the crack 2*a*, the complete Westergaard function should be used without Irwin's simplification that generated $K_I = \sigma_n\sqrt{(\pi a)}$. In this way, given $z = x + i\cdot y$, $Z(z) = z\sigma_n/\sqrt{(z^2 - a^2)}$ and $Z'(z) = -a^2\sigma_n/(z^2 - a^2)^{3/2}$, where *Z*(*z*) is the Westergaard function that solves the problem of a plate submitted to the biaxial nominal stresses $\sigma_x(z \to \infty) = \sigma_y(z \to \infty) = \sigma_n$, then

$$\begin{cases} \sigma_x = Re(Z) - y\,Im(Z') - \sigma_n \\ \sigma_x = Re(Z) + y\,Im(Z') \\ \tau_{xy} = -y\,Re(Z') \end{cases} \tag{20}$$

are the stresses that act on the plate under uniaxial traction (in the same way as in Williams' series, a constant term can be added to the σ_x component to satisfy the contour conditions in this case). Representing *Z* and *Z'* in polar coordinates centered at the crack tip, then

$$\begin{cases} Z = \dfrac{[a+(r\cdot\cos\theta)+i(r\cdot\sin\theta)]\cdot\sigma_n}{\sqrt{[a+(r\cdot\cos\theta)+i(r\cdot\sin\theta)]^2-a^2}} \\ Z' = \dfrac{-a^2\cdot\sigma_n}{\left\{[a+(r\cdot\cos\theta)+i(r\cdot\sin\theta)]^2-a^2\right\}^{3/2}} \end{cases} \tag{21}$$

To obtain the estimate of the elastoplastic border from Mises under plane stress, it is sufficient to substitute Eq. (21) into (20) and to use an equation similar to (18) to obtain

$$\begin{aligned} &\left\{\left[Re\left(\frac{(a+r\cdot\cos\theta+i\cdot r\sin\theta)\cdot\sigma_n}{\sqrt{(a+r\cdot\cos\theta+i\cdot r\sin\theta)^2-a^2}}\right)-y\,Im\left(\frac{-a^2\cdot\sigma_n}{\left[(a+r\cdot\cos\theta+i\cdot r\sin\theta)^2-a^2\right]^{3/2}}\right)-\sigma_n\right]^2+\right.\\ &+\left[Re\left(\frac{(a+r\cdot\cos\theta+i\cdot r\sin\theta)\cdot\sigma_n}{\sqrt{(a+r\cdot\cos\theta+i\cdot r\sin\theta)^2-a^2}}\right)+y\,Im\left(\frac{-a^2\cdot\sigma_n}{\left[(a+r\cdot\cos\theta+i\cdot r\sin\theta)^2-a^2\right]^{3/2}}\right)\right]^2-\\ &-\left[Re\left(\frac{(a+r\cdot\cos\theta+i\cdot r\sin\theta)\cdot\sigma_n}{\sqrt{(a+r\cdot\cos\theta+i\cdot r\sin\theta)^2-a^2}}\right)-y\,Im\left(\frac{-a^2\cdot\sigma_n}{\left[(a+r\cdot\cos\theta+i\cdot r\sin\theta)^2-a^2\right]^{3/2}}\right)-\sigma_n\right]\cdot\\ &\cdot\left[Re\left(\frac{(a+r\cdot\cos\theta+i\cdot r\sin\theta)\cdot\sigma_n}{\sqrt{(a+r\cdot\cos\theta+i\cdot r\sin\theta)^2-a^2}}\right)+y\,Im\left(\frac{-a^2\cdot\sigma_n}{\left[(a+r\cdot\cos\theta+i\cdot r\sin\theta)^2-a^2\right]^{3/2}}\right)\right]+\\ &\left.+3\cdot\left[-y\,Re\left(\frac{-a^2\cdot\sigma_n}{\left[(a+r\cdot\cos\theta+i\cdot r\sin\theta)^2-a^2\right]^{3/2}}\right)\right]^2\right\}^{1/2}-S_y=0 \end{aligned} \tag{22}$$

This equation can be solved by numerical methods using similar techniques as the ones used in Eq.(18): for each value of θ, the value of *r* that satisfies Eq.(22) is obtained, locating the desired border. This process is computationally intensive, but it can be easily repeated to consider also the case of plane strain, generating Figs. 4(a) and 4(b).

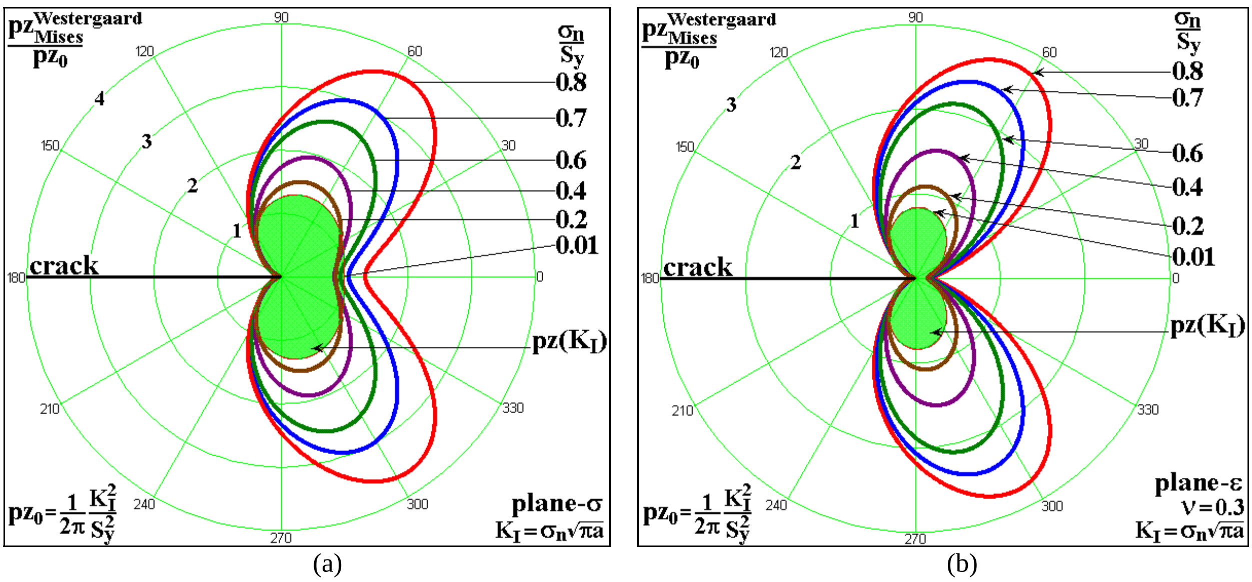

Fig. 4: Plastic zones around the crack tip modeled using the complete Westergaard stress function under: (a) plane stress; (b) plane strain.

5. COMPARISON BETWEEN THE INGLIS AND WESTERGAARD SOLUTIONS

Figures 5 and 6 compare the plastic zones estimated from Inglis, assuming (i) that the crack is an Inglis' hole with tip radius equal to half the *CTOD* associated with K_I; and (ii) using the complete Westergaard function, without the simplification that Inglis used to obtain K_I. The near overlapping of these two curves, which were generated from totally different equations, certainly it is not coincidental. This indicates that the predicted large effect of σ_n on the plastic zone size and shape is true.

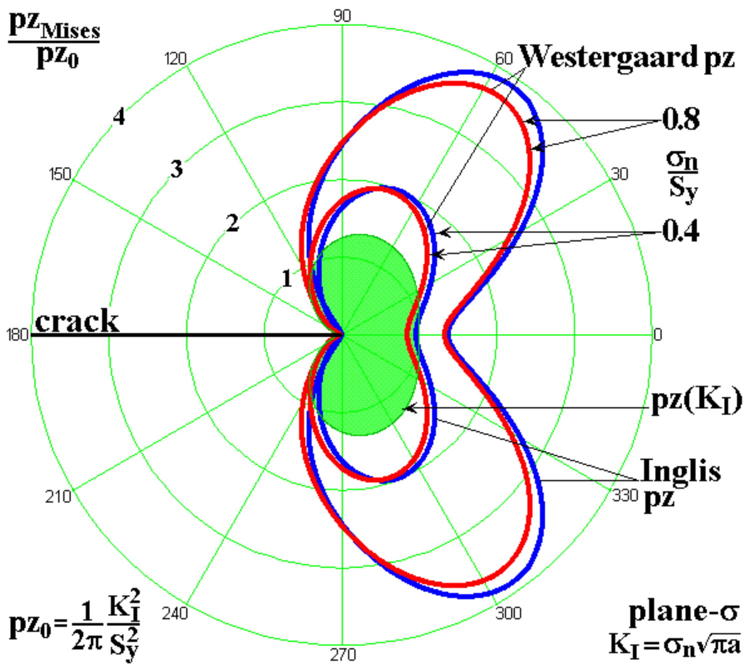

Fig. 5: Comparison between the plastic zones estimated from Inglis and from Westergaard, under plane stress.

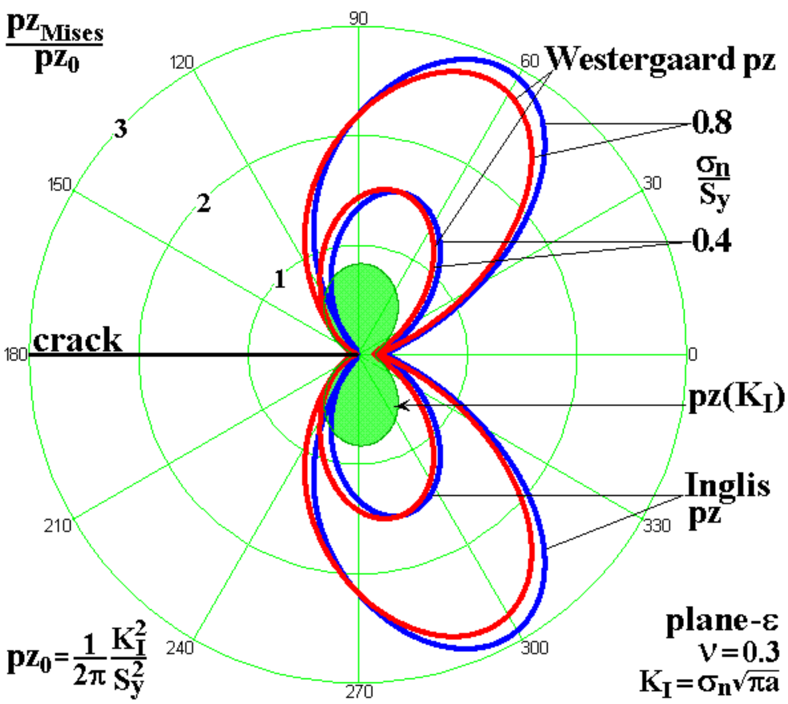

Fig. 6: Comparison between the plastic zones estimated from Inglis and from Westergaard, under plane strain.

This point should be emphasized. It is the size of the plastic zone that validates the LEFM predictions. And it is very convenient to assume that this size only depends on K_I, as it is traditionally assumed in all the textbooks on this subject. However, both the size and shape of the plastic zone also depend on the magnitude of the applied nominal stress. And for nominal stresses of the order of those usually used in mechanical components, the estimated plastic zones considering the effect of σ_n are much larger than the traditional plastic zone estimates that only depend on K_I. In addition, the effect of σ_n also depends on the shape of the component. In this work, only an infinite plate is analyzed, but the effect of the component shape is also very significant. This can be used to explain a series of incongruities in the LEFM predictions.

It is interesting to note that the coincidence of the plastic zones estimated from Inglis and from Westergaard can be forced simply by changing the estimate of the Inglis' notch radius. Instead of assuming a tip radius of $\rho = CTOD/2$, the smaller semi-axis b can be assumed as equal to $CTOD/2$, resulting in Fig. 7, for plane stress. Note in this figure how well both estimates agree. The agreement is also excellent under plane strain.

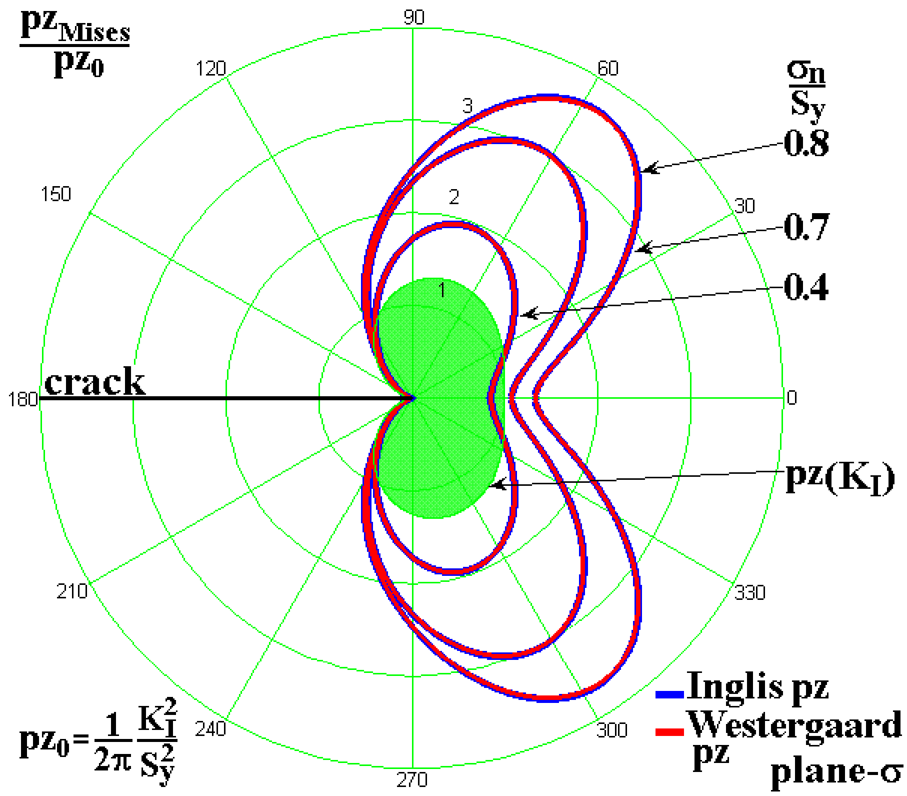

Fig. 7: Agreement of the plastic zones estimated by Inglis (assuming $b = CTOD/2$) and Westergaard under plane stress.

6. CONCLUSIONS

The nominal stress significantly affects the size and shape of the plastic zones ahead of cracks in an Inglis (infinite) plate. Therefore, unlike what is usually accepted and taught in the traditional LEFM literature, the plastic zones do not depend only on the magnitude of the stress intensity factor K_I. This fact has important consequences, because it can be used to question the similarity principle, one of the pillars of the mechanical design methods against fracture. Therefore, this effect should be better explored and understood.

7. REFERENCES

Anderson,T.L., 2005, "Fracture Mechanics", 3rd ed., CRC.
Barson, J.M., 1987, "Fracture Mechanics Retrospective", ASTM.
Barson, J.M. and Rolfe, S.T., 1999, "Fracture and Fatigue Control in Structures", 3rd ed., ASTM.
Broek, D., 1986, "Elementary Engineering Fracture Mechanics", 4th ed., Kluwer.
Broek, D., 1988, "The Practical Use of Fracture Mechanics", Kluwer.
Gdoutos, E.E., 2006, "Fracture Mechanics, An Introduction", 2nd ed., Springer.

Sanford, R.J., 1997, "Selected Papers on Linear Elastic Fracture Mechanics", SEM.
Sanford, R.J., 2003, "Principles of Fracture Mechanics", Pearson Education.
Unger, D.J., 2001, "Analytical Fracture Mechanics", Dover.
Whittaker, B.N., Singh, R.N. and Sun, G., 1992, "Rock Fracture Mechanics", Elsevier.

8. RESPONSIBILITY NOTICE

The authors are the only responsible for the printed material included in this paper.